

The structural properties of LaRO_3 ($\text{R}=\text{Cr}, \text{Mn}, \text{Fe}$): a first-principles calculation

Y. R. Li¹, Z. T. Hou¹, T. X. Wang², Y. Li^{1,*}, H. Y. Liu¹, X. F. Dai¹, G. D. Liu¹

¹ School of Material Science and Engineering, Hebei University of Technology, Tianjin 300130, China

² College of Physics and Information Engineering, Henan Normal University, 453007 Xinxiang, China

E-mail: liyingphy@126.com

Abstract. We investigate the structural properties of three lanthanum transition-metal oxides (LaRO_3 , $\text{R}=\text{Cr}, \text{Mn}, \text{Fe}$) by the first-principles method based on density functional theory. The crystal parameters and electronic structures are calculated for three different oxides. The results show that the magnitude of lattice distortion is the strongest in LaMnO_3 , and the slightest in LaCrO_3 among three compounds. The magnetic ground states of LaCrO_3 and LaFeO_3 are G-type antiferromagnet. However, for LaMnO_3 , GGA+U fails to predict the experimental ground state, and only the internal coordinates are relaxed and the experimental lattice constants are fixed, the LDA+U can reproduce the experimental A-type antiferromagnetic state. It is found that Fe-3d electrons in LaFeO_3 occupy the localized orbital with the low energy, while Cr-3d and Mn-3d electrons in LaCrO_3 and LaMnO_3 occupy the relatively wide energy states due to the strong hybridization between d electrons and p electrons of oxygen atoms.

1. Introduction

Lanthanum transition-metal oxides LaRO_3 ($\text{R}=\text{Cr}, \text{Mn}, \text{Fe}$) display a complex correlation among structural, orbital, magnetic, and electronic degrees of freedom due to the existence of strongly correlated effect between 3d electrons of transition metal atoms. Over the past decades, LaRO_3 compounds have been widely investigated because of their technical importance and the fundamental interest in the physics of their phase transition [1, 2, 3, 4, 5, 6, 7, 8]. Among these oxides, LaMnO_3 had attracted considerable attention due to its colossal magnetoresistance, a large variety of phases with remarkably different structural, magnetic and transport properties [9, 10], and a large Jahn-Teller (JT) effect [11, 12]. The Jahn-Teller effect is often encountered in octahedral complexes of the transition metals, and caused mainly by the presence of molecular orbital of the 3d transition metals [13].

In the present work, we systematically investigate the structural properties and Jahn-Teller lattice distortion for three types of oxides LaCrO_3 , LaMnO_3 , and LaFeO_3 by the first-principles calculation based on density functional theory. The magnetic ground state and spin density of states of three oxides are also studied.



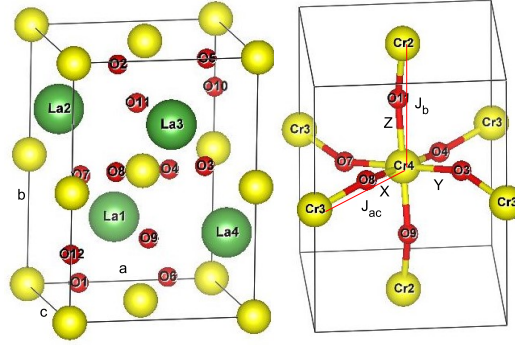


Figure 1. The orthogonal supercell model of LaRO_3 (left panel), where the red sphere is O atom, the green sphere is La atom, and the yellow sphere is the transition metal atom. The right panel displays a partition of orthogonal supercell (here take LaCrO_3 for example), where J_{ac} represents the exchange interaction parameter between the nearest-neighbor Cr3 and Cr4 atoms in the ac plane and J_b exchange interaction parameter between next nearest-neighbor Cr2 and Cr4 atoms. The X, Y, and Z represent the direction of different R-O bonds.

2. Computational details

In this paper, the first-principles calculation based on density functional theory (DFT) is performed by using the Vienna Ab initio Simulation Package (VASP). The interactions between ions and electrons are described by the projector augmented wave (PAW) method developed by Blöchl [14, 15]. The cut-off energy of the plane-wave basis is set to be 650 eV, and the Brillouin-zone integration is applied by $8 \times 8 \times 8$ Monkhorst-Pack special k-points. All atoms are fully relaxed with the total energy change less than 10^{-6} eV and the force on each ion less than 0.01 eV. The La-5s²5p⁶5d¹6s², O-2s²2p⁴, Cr-3p⁶3d⁵4s, Mn-3p⁶3d⁵4s², Fe-3p⁶3d⁶4s² are considered as valence electrons. The strong correlation effects of 3d electrons are treated by GGA+U with the Perdew-Bruke-Ernzerhof (PBE) potential. The values of U_{eff} (U-J) are taken as 5 eV for three compounds. For LaMnO_3 , we also compute the total energy and electronic structure using the LDA exchange correlation potential.

In the calculation, we use $\sqrt{2} \times \sqrt{2} \times 2$ orthogonal supercell containing 4 transition metal atoms, 4 La atoms, and 12 oxygen atoms, as shown in Fig. 1. For the convenience of analysis, we also display a partition of orthogonal supercell in the right panel of Fig. 1, where the central atom Cr4, its neighboring atoms Cr2 and Cr3, and six oxygen atoms (O3, O4, O7, O8, O9, O11) around Cr4 are clearly seen. The experimental values of lattice constants parameters are taken as $a = 5.508$ Å, $b = 7.791$ Å, $c = 5.484$ Å for LaCrO_3 [16], $a = 5.705$ Å, $b = 7.703$ Å, $c = 5.536$ Å for LaMnO_3 [17], and $a = 5.569$ Å, $b = 7.885$ Å, $c = 5.530$ Å for LaFeO_3 [18].

3. Results and discussions

3.1. The magnetic ground state

To find the magnetic ground state, we first carry out the full structural optimization for LaCrO_3 , LaMnO_3 , and LaFeO_3 in the case of four magnetic configurations, i.e., ferromagnetic (FM), A-type antiferromagnetic (A-AFM), G-type antiferromagnetic (G-AFM), and C-type antiferromagnetic (C-AFM) states, as sketched in Fig.2, and calculate their total energies and magnetic moments, which are shown in Table 1. The magnetic ground states of LaCrO_3 and LaFeO_3 are found to be G-AFM state, which is in agreement with the experiment [7]. For LaRO_3 , the result shows that LaMnO_3 has lower energy in FM state than in A-AFM state by GGA+U, as in previous calculations [19, 20, 21, 22]. And if only the internal coordinates with the

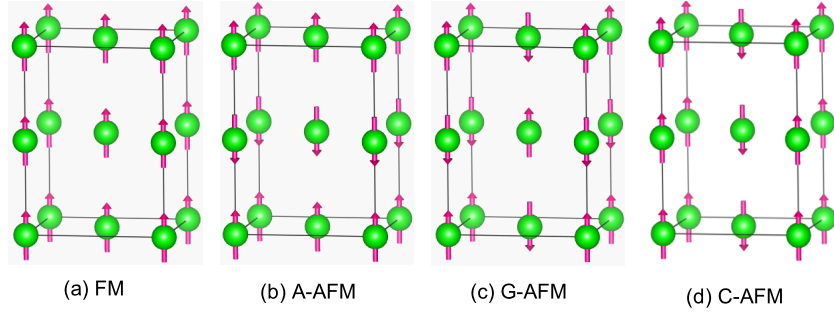


Figure 2. Four types of magnetic configurations of transition-metal atoms R in LaRO_3 (a) FM, (b) A-AFM, (c) G-AFM, and (d) C-AFM, where La and O atoms are removed for clarity and the green sphere represents R atoms.

experimental lattice constants are optimized by using LDA+U exchange correlation potential, we can reproduce the experimental ground state with A-type antiferromagnetic ordering. According to the energy difference, we derive the exchange coupling parameters J_{ac} (J_b) between R4 and R3 (R2)(see Fig.1 (b)), and simulate the magnetic transition temperature by Monte Carlo method [23], also given in Table 1. For comparison, the experimental transition temperature is also given in Table 1. Our simulated magnetic transition temperature $T = 79(550)$ K for LaCrO_3 (LaFeO_3) are lower than 290(750) K of the experimental values [24, 25, 26], which should be attributed to the U values and computational accuracy. For LaMnO_3 , it is found that the magnetic moment of $3.75\mu_B$ obtained from LDA is in agreement with the experimental one of $3.7\mu_B$ [27], and the out-of-plane magnetic coupling parameter of -1.85 meV is lower than experimental one of -1.2 meV [28].

Table 1. The total energy of different magnetic states with respect to FM state, the magnetic moment of the transition-metal atom for the stable configurations, the exchange parameters, and the magnetic transition temperature of LaCrO_3 , LaMnO_3 , and LaFeO_3 .

	LaCrO_3	$\text{LaMnO}_3\text{-GGA (LDA)}$	LaFeO_3
FM	0	0 (0)	0
A-AFM(meV)	-34.98	58.4 (-56.1)	-287.45
G-AFM(meV)	-113.66	305.46 (-)	-798.39
C-AFM(meV)	-80.79	256.59 (-)	-570.31
$m_R(\mu_B)$	2.95	3.9(3.75)	4.23
$J_{ac}(\text{meV})$	2.214	3.86 (-1.75)	5.4
$J_b(\text{meV})$	1.884	1.825 (-)	5.155
$T_N(\text{K})$	79	203	550

3.2. Structure parameters

The degree of Jahn-Teller distortion can be reflected by three R-O bond lengths and R-O-R bond angles in RO_6 octahedron. In Table 2 we present the equilibrium lattice constants, normal mode [22], R-O bond lengths, O-R-O bond angle, and also R-O-R bond angles for G-AFM LaCrO_3 , A-AFM LaMnO_3 , and G-AFM LaFeO_3 . The lattice constants after structure optimization are

Table 2. The calculated equilibrium lattice constants, bond lengths, and bond angles for LaCrO₃, LaMnO₃, and LaFeO₃.

structure	method	a(Å)	b(Å)	c(Å)	Q_2	Q_3
LaCrO ₃	our work	5.6139	7.8942	5.5702	0.0014	0.0041
	[29]	5.523	7.801	5.527		
	[30]	5.483	7.765	5.520		
	[16]	5.501	7.791	5.484		
LaMnO ₃	our work	5.765	7.582	5.429	0.0764	0.425
	[29]	5.623	7.814	5.528		
	[27]	5.742	7.668	5.532		
	[17]	5.7046	7.7029	5.5353		
LaFeO ₃	our work	5.6431	7.9146	5.5772	0.0057	0.316
	[29]	5.597	7.860	5.551		
	[31]	5.565	7.854	5.557		
	[18]	5.569	7.855	5.53		
	[7]	5.563(5)	7.850(8)	5.553(3)		
	[8]	5.542	7.856	5.5596		
	LaCrO ₃	LaMnO ₃	LaFeO ₃			
bond length (Å)						
R-O3(O7)	2.029	2.151	2.041			
R-O4(O8)	2.027	1.915	2.03			
R-O9(O11)	2.026	1.949	2.034			
bond angle (°)						
O3(O7)-R-O4(O8)	91.15	89.14	91.04			
O3(O7)-R-O11	89.49	91.82	89.35			
O4(O8)-R-O11	88.92	90.87	88.71			
R3-O7-R4	154.32	153.68	154.03			

a bit larger than the experimental data for three compounds. In LaCrO₃, three bond lengths, i.e., Cr4-O3 (O7), Cr4-O4 (O8), Cr4-O9 (O11), are nearly equal, and the relative ratio of bond length in the Y direction to the X (Z) direction is 0.098% (0.148%). In comparison, in LaMnO₃ the bond length in the Y direction is obviously larger than that in the X (Z) directions with relative ratio 10.97% (9.39%). For LaFeO₃ the bond length in the Y direction is slightly larger than that in the X (Z) directions with relative ratio 0.544% (0.368%).

Moreover, we measure the magnitude of JT distortion by calculating the normal mode parameters $Q_2 = (1/\sqrt{2})(X1 - X4 - Y2 + Y5)$ and $Q_3 = (1/\sqrt{6})(2Z3 - 2Z6 - X1 + X4 - Y2 + Y5)$ [12, 32], where X,Y,Z directions are marked in Fig.1. The Q_2 and Q_3 of LaMnO₃ is larger than those of LaCrO₃ and LaFeO₃, as shown in Table 2. For three compounds, the bond angles, i.e., O3 (O7)-R-O4 (O8), O7-R-O11, O8-R-O11, have a slight deviation from the perpendicular angles each other. All above results indicate that the lattice distortion of LaMnO₃ is the most pronounced, LaFeO₃ is relatively slight, and the JT distortion of LaCrO₃ is almost ignorable. Additionally, the R-O-R bond angles exhibit a large deviation from the 180 degree in the perovskite structure, which also suggests the occurrence of structural distortion. The JT distortion can also be further explained by the electronic structure of 3d electrons in transition metal atoms.

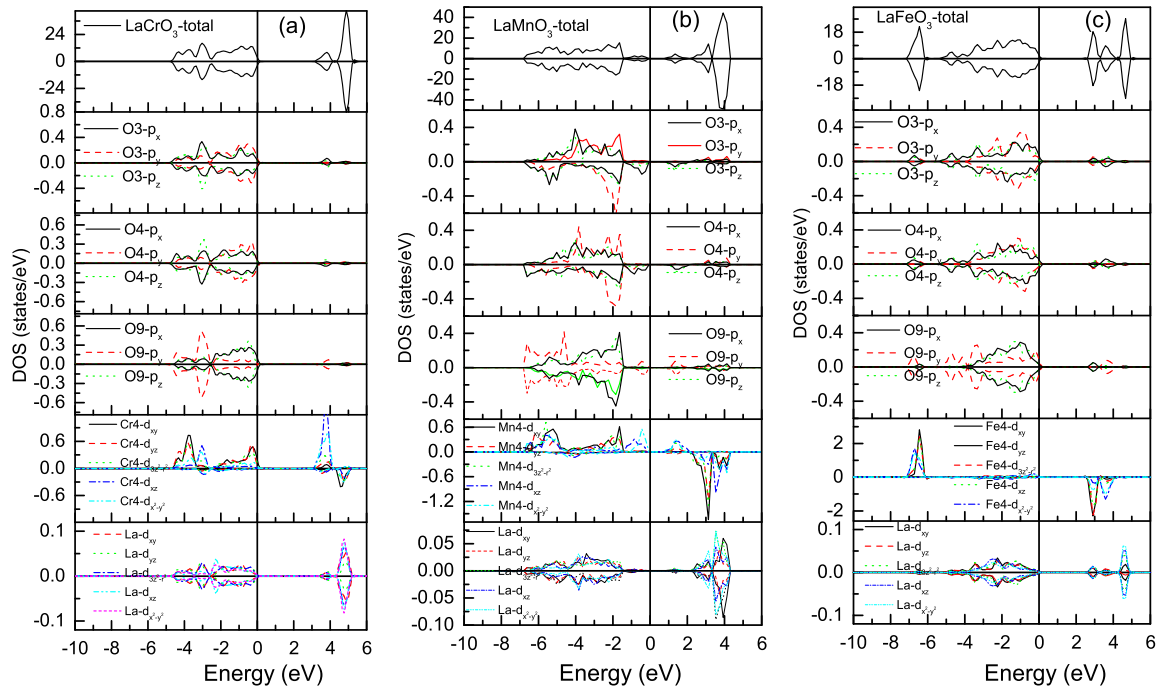


Figure 3. The total and partial density of states for O-p, Cr-d, La-d electrons in (a) LaCrO₃, (b) LaMnO₃, and (c) LaFeO₃.

3.3. Electronic structure

Fig.3 shows the total and partial density of states (DOS) for G-AFM-LaCrO₃, A-AFM-LaMnO₃, and G-AFM-LaFeO₃. It is found that three types of compounds are semiconductor. The LaCrO₃ has the largest energy gap of 3.1 eV, the energy gap of LaMnO₃ is 0.875 eV, close to other calculated results of 0.90 eV [22], and that of LaFeO₃ is 2.56 eV. The partial density of states of R atoms, three types of O atoms around it, and one La atom in three compounds are presented in Figs. 3 (a), 3 (b) and 3 (c), respectively, in order to clarify the orbital hybridization and ligand change around R atoms. We can see that the valence energy states are mainly contributed by the R-3d and O-2p electrons with a small contribution of La-5d electrons. There exists strong orbital hybridization between O-2p electrons and Cr (Mn)-3d electrons in LaCrO₃ (LaMnO₃).

For LaCrO₃ and LaFeO₃, three p orbitals of O3 and O4 atoms in the XY plane exhibit a slight exchange splitting, while no exchange splitting is found for three p orbitals of O9 atom along the Z direction (see Figs. 3 (a) and 3 (c)). In comparison, the p orbitals of O3 and O4 atoms in LaMnO₃ have obvious exchange splitting, and three p orbitals of O9 atom are also slightly asymmetry, as shown in Fig. 3 (b). Under the action of the octahedron crystal field with low symmetry, three Cr4-d electrons in LaCrO₃ do not apparently occupy the d_{xy} , d_{yz} , d_{xz} orbitals. The d electrons of Mn atom also occupy widely the five orbitals, i.e., d_{xy} , d_{yz} , d_{xz} , $d_{3z^2-r^2}$, $d_{x^2-y^2}$, due to the strong hybridization between 3d electrons and 2p electrons of O atoms.

In addition, it is found that the valence energy states of LaFeO₃ are separated into two parts. The energy states ranging from -8 eV to -6 eV are contributed by Fe-3d electrons and small O-2p electrons, and those from -5 eV to 0 eV are contributed by O-2p electrons and La-5d electrons. Compared with that of LaCrO₃ and LaMnO₃, the orbital hybridization of LaFeO₃ between O-2p and Fe-3d electrons becomes weak. The Fe-d electrons orbital in LaFeO₃ is very localized and has a small energy scale ranging from -7.1 eV to -6.1 eV due to small orbital hybridization between Fe-3d electrons and O-2p electrons.

4. Conclusions

In summary, we have investigated the magnetic ground state, structure parameters, electronic density of states in LaCrO_3 , LaMnO_3 and LaFeO_3 by the first-principles calculation. The results show that the magnetic ground states of LaCrO_3 and LaFeO_3 are G-type antiferromagnetic state, which is in agreement with the experimental results. For LaMnO_3 , it is found that the ferromagnetic ground state has lower energy than the antiferromagnetic state in the case of optimizing both internal coordinates and lattice constants based on GGA+U, and the A-type antiferromagnetic state can be obtained if only optimizing the internal coordinates with the experimental lattice constants based on LDA+U. The lattice distortion of LaMnO_3 is the most pronounced among three compounds. Compared with the d electrons in LaCrO_3 and LaMnO_3 , the d electrons in LaFeO_3 have small energy splitting and occupy the very localized orbital.

5. Acknowledgement

This work is funded by the National Nature Science Foundation of China (Grant Nos. 11204064 and U1304518)

References

- [1] Jiang S, Liu L, Ong K, Wu P, Li J, Pu J 2008 *Power Sources* **176** 82
- [2] Nithya V, Immanuel R, Senthilkumar S, Sanjeeviraja C, Perelshtein I, Zitoun D, Selvan R 2012 *Mater. Res. Bull.* **47** 1861
- [3] Nakayama S 2001 *Mater. Sci.* **36** 5643
- [4] Zhou J, Alonso J, Muoz A, Fernandez-Daz M, Goodenough J 2011 *Phys. Rev. Lett.* **106** 057201
- [5] Scafetta M, Cordi A, Rondinelli J, May S 2014 *Phys. Condens. Matter* **26** 505502
- [6] Taran O, Ayusheev A, Ogorodnikova O, Prosvirin I, Isupova L, Parmon V 2016 *Applied Catalysis B: Environmental* **180** 86
- [7] Mahapatra A, Mitra A, Mallick A, Ghosh M, Chakrabarti P 2016 *Materials Letters* **169** 160
- [8] Chanda S, Saha S, Dutt A, Irfan B, Chatterjee R, Sinha T.P. 2015 *Journal of Alloys and Compounds* **649** 1260
- [9] Zenia H, Gehring G, Temmerman W 2005 *New J. Phys.* **7** 257
- [10] Banach G, Temmerman W 2004 *Phys. Rev. B* **69** 054427
- [11] Dagotto E, Hotta T, Moreo A 2001 *Phys. Rep.* **344** 1
- [12] Hou Y, Xiang H, Gong X 2014 *Phys. Rev. B* **89** 064415
- [13] Brien O, Mary C, Chancey C 1993 *Am. J. Phys.* **61** 688
- [14] Blochl P 1994 *Phys. Rev. B* **50** 17953
- [15] Kresse G, Joubert J 1999 *Phys. Rev. B* **59** 1758
- [16] Tolochko S, Kononyuk I, Zonov Y, Ivashkevich L 1987 *Inorg. Mater.* **23** 743
- [17] Krogh I, Krogh A, Norby P, Skou E 1994 *Solid State Chem.* **113** 320
- [18] Iguchi E, Jung W 1994 *Phys. Soc. Jpn.* **63** 3078
- [19] Sawada H, Morikawa Y, Terakura K, Hamada N 1997 *Phys. Rev. B* **56** 12154
- [20] Sawada H, Terakura K 1998 *Phys. Rev. B* **58** 6831
- [21] Kotomin E, Evarestov R, Mastrikov Y, Maier J 2005 *Phys. Chem.* **7** 2346
- [22] Hashimoto T, Ishibashi S, Terakura K 2010 *Phys. Rev. B* **82** 045124
- [23] Li Y, Liu B 2006 *Phys. Rev. B* **73** 174418
- [24] Tiwari B, Dixit A, Naik R, Lawes G and Ramachandra Rao M 2014 *Materials Research Express* **2** 2
- [25] Hearne G, Pasternak M 1995 *Phys. Rev. B* **51** 11495
- [26] Mahapatra A, Mitra A, Mallick A, Ghosh M, Chakrabarti P 2016 *Materials Letters* **169** 160
- [27] Elemans J, Van Laar B, Van Der Veen K, Loopstra B 1971 *J. Solid State Chem.* **3** 238
- [28] Moussa F, Hennion M, Rodriguez-Carvajal J, Moudén H, Pinsard L, Revcolevschi A 1996 *PRB* **54** 15149
- [29] Wang Y and Cheng H. 2013 *J. Phys. Chem. C* **117** 2106
- [30] Khattak C, Cox D 1977 *Mater. Res. Bull.* **12** 463
- [31] Dann S, Currie D, Weller M, Thomas M, Al-Rawwas A 1994 *J. Solid State Chem.* **109** 134
- [32] Kanamori J 1960 *J. Appl. Phys.* **31** 14S